



1 **Comment on:**

2

3 **Macroscopic water vapor diffusion is not enhanced in snow**

4

5 **Andrew C. Hansen**

6

7 Professor Emeritus, University of Wyoming, Laramie, WY 82071 USA

8

9 *Correspondence to:* A.C. Hansen (hansen@uwyo.edu)

10 December 2021

11

12 **Abstract**

13

14 The central thesis of the authors' paper is that macroscopic water vapor diffusion is not enhanced
15 in snow compared to diffusion through humid air alone. Further, mass diffusion occurs entirely as the
16 result of water vapor diffusion in the humid air at the microscale and the ice phase has no effect other than
17 occupying volume where diffusion cannot occur. The foundation of their conclusion relies on the premise
18 that the synchronous sublimation and deposition of water vapor across ice grains, known as hand-to-hand
19 water vapor transport, does not lead to enhanced mass diffusion. We use a layered microstructure to
20 rigorously show that diffusion is enhanced at all ice volume fractions compared to diffusion through
21 humid air alone, and further, the hand-to-hand model of diffusion correctly predicts this diffusion
22 enhancement.

23

24 The authors attempt to dismiss the concept of enhanced mass transfer resulting from hand-to-
25 hand water vapor transport by arguing that there is a "counterflux" of water vapor in the form of
26 downward motion of ice. While the ice phase *appears* to be propagating downward, all continuum
27 material points of water (either vapor or ice) are moving upward (counter to the temperature gradient)
28 with a monotonically increasing (nonnegative) motion. Specifically, material points of water in vapor
29 form are diffusing upward through the humid air while material points of water in the form of ice are at
30 zero velocity while locked in the ice phase. Material points of water never exhibit downward motion,
31 despite the ice phase *appearance* of downward motion. *Since the motion of all material points of water is*
32 *monotonically increasing for all time, there is no counterflux of mass due to downward motion of the ice*
33 *and such apparent motion is a mirage in the context of mass transfer.*

34 This paper presents a rigorous fluid mechanics control volume analysis of mass transfer to
35 demonstrate that the hand-to-hand model of diffusion produces the correct diffusion coefficient for the
36 layered microstructure. Moreover, the control volume analysis shows why the authors' approach of
37 volume averaging the microscale diffusion coefficient does not capture the complete water vapor mass
38 transport and therefore does not produce the correct macroscale diffusion coefficient.

39 An entirely fresh perspective on the role of the ice phase in mass diffusion is also presented. In
40 particular, an analysis showing diffusion enhancement is developed without resorting to the hand-to-hand
41 diffusion analogy. In brief, rather than looking at the ice as blocking microscale diffusion, the ice phase
42 should be viewed as a reservoir of water, containing vast amounts of water vapor, ready to be released in
43 the diffusion process.

44 In conclusion, mass diffusion in a layered microstructure is enhanced at all ice volume fractions
45 compared to diffusion through humid air as a pure substance. The mechanism producing this enhanced
46 diffusion is also on full display in snow under strong temperature gradients. Hence, it is entirely possible,
47 indeed probable, that macroscopic water vapor diffusion is enhanced in snow compared to diffusion in
48 humid air as a pure substance.



49 **1. Introduction**

50

51 Heat and mass transfer at the macroscale of a snow cover is a complex phenomenon, even under
52 the simplest of conditions. The challenges in modeling thermophysical processes in snow stem from the
53 fact that snow is a phase changing mixture of ice and humid air. Under a macroscale temperature
54 gradient, the transport properties for snow are influenced by water vapor diffusion. Diffusion is, in turn,
55 influenced by several microscale factors including elevated temperature gradients in the humid air as well
56 as the complex 3D topology of the ice phase. However, without question, the most vexing aspect of
57 modeling diffusion is the condensation and sublimation of water molecules resulting in “hand-to-hand”
58 water vapor transport as famously described by Yosida (1955).

59

60 Figure 1 shows two forms of water vapor transport in snow under the influence of a macroscale
61 temperature gradient. Some water vapor molecules follow paths around ice grains while others undergo
62 sublimation and condensation, resulting in the hand-to-hand vapor transport described by Yosida. While
63 the existence of hand-to-hand water vapor transport is well known for some 60+ years, there remains
64 controversy surrounding the relation of this mass transfer mechanism to the diffusion coefficient of
65 snow.

66

67 Let D_{v-a} represent the binary diffusion coefficient of water vapor in air. One view of mass
68 transfer in snow is that water vapor diffusion is driven by the local (microscale) temperature gradient in
69 the humid air constituent. Since the phase transitions that take place at the microscale serve as a temporal
70 storage of vapor in the form of ice, they should, in principle, reduce the effective water vapor transport,
71 and therefore reduce the effective diffusion coefficient. The work of Giddings and LaChapelle (1962),
72 Calonne et al. (2014), Shertzer and Adams (2018), and Fourteau et al. (2021a, 2021b) follow this line of
73 reasoning. In brief, they adopt the view

74

$$D_s < D_{v-a} .$$

75 An alternate perspective of mass transfer in snow is that hand-to-hand vapor transport resulting
76 from sublimation and deposition of water vapor is a transport mechanism contributing to the diffusion
77 coefficient, D_s . In this context, the ice phase is viewed as a near instantaneous source/sink of water vapor
78 transport, thereby shortening diffusion paths through the humid air and enhancing diffusion rates. The key
79 attribute of this reasoning is that water vapor molecules are indistinguishable from one another. Water
80 vapor condensing on the bottom of an ice grain is identical, in form, to water vapor sublimating off the
81 top of an ice grain. Prior research advocating this position may be found in Yosida (1955), Sommerfeld
82 (1982), Colbeck (1993), and Hansen (2019). This approach suggests that, for low density snow, the
83 diffusion coefficient for snow lies close to the diffusion coefficient for humid air alone with perhaps a
84 slight enhancement under strong temperature gradients (Hansen, 2019).

85

86 The paper begins with a comparison of the mathematical framework of the two approaches to the
87 diffusion coefficient outlined above. The comparison is presented in the context of a layered
88 microstructure of ice and humid air, Figure 2. The layered microstructure represents an ideal
89 microstructure to study in that hand-to-hand water vapor transport plays a dominant role in mass transfer.
90 In addition, an analytical solution for the energy flux exists—a solution based only on one-dimensional
91 heat and mass transfer principles with a long history of supporting development.

92

93 Next, a rigorous control volume analysis of balance of mass is performed as an independent
94 calculation of the diffusion coefficient. The control volume analysis brings to light three important
95 results: i) the hand-to-hand model of diffusion correctly predicts the diffusion coefficient, ii) volume
96 averaging the local (microscale) mass flux, as presented in Fourteau et al. (2021a), does not capture the

97 total transport of water moving through the system, and iii) diffusion is enhanced at all ice volume
98 fractions compared to diffusion through humid air alone.

99
100 While the hand-to-hand diffusion analogy is elegant and incredibly valuable in properly modeling
101 mass diffusion, the fundamental criticism remains that the proposed diffusion mechanism, as put forth by
102 Yosida (1955), “is not physically sound” (Fourteau et al., 2021a). An entirely fresh perspective on
103 diffusion is provided where hand-to-hand water vapor transport is dispensed with as a diffusion
104 mechanism while achieving the same results. In brief, rather than looking at the ice as blocking
105 microscale diffusion, the ice phase should be viewed as a reservoir of water vapor existing within the
106 material. Remarkable clarity on mass diffusion in ice/humid air mixtures is achieved in an entirely
107 different light.

108
109 Hand-to-hand vapor transport is also an important mechanism of mass transfer in snow as,
110 without it, there would be no temperature gradient metamorphism. Hence, the layered microstructure
111 provides a foundational guide as to how to move forward in studying thermophysical processes in snow.

112
113

114 2. Ground truths

115

116 In this section, two topics are introduced that provide a valuable foundation for the heat and mass
117 transfer analysis that follows. The results are noncontroversial and simply represent ground truths
118 necessary to move forward.

119

120 Some basic assumptions are also introduced that are assumed to hold at all times, including:

121

122 • Infinitely fast surface kinetics for deposition and sublimation of water vapor are assumed
123 for the layered microstructure of ice and humid air

124

125 • The humid air is saturated

126

127 • Convection and radiation are neglected

128

129 2.1 Defining the mass flux

130 To begin, a few comments about the nature of flux vectors in general are appropriate. In physics
131 and applied mathematics, the flux of a vector quantity represents the amount of the vector field passing
132 through a surface per unit of area per unit of time. Specifically, referring to Figure 3, if \mathbf{n} defines a unit
133 normal for the differential surface, dS , and \mathbf{F} is a vector field, the flux through the surface is a scalar
134 given by

$$135 \quad \text{Flux} = \int_{\partial\mathcal{R}} \mathbf{F} \cdot \mathbf{n} \, dS \quad , \quad (1)$$

136 where $\partial\mathcal{R}$ defines the surface. Examples of flux are numerous in mechanics and include phenomena such
137 as mass flux, momentum flux, and kinetic energy flux. The *flux of mass across the boundary* $\partial\mathcal{R}$ is of
138 interest here, i.e., let $\mathbf{F} = \rho\mathbf{v}$

139

$$140 \quad \text{mass flux} = - \int_{\partial\mathcal{R}} \rho \mathbf{v} \cdot \mathbf{n} \, dS \quad . \quad (2)$$

141

142 The minus sign in the above simply indicates mass is leaving the region \mathcal{R} .

143



144 Now return to Figure 2(a), showing the homogenized layered microstructure in the presence of a
145 temperature gradient, bounded by solid ice blocks held at fixed temperatures. The mass flux across the
146 upper boundary of the layered microstructure is the amount of mass passing through the upper surface per
147 unit of area per unit of time. Physically, it is the amount of water vapor turning to ice at the solid
148 ice/humid air boundary. Note that a humid air layer within the layered microstructure always lies adjacent
149 to the solid ice block.

150

151 As time proceeds, ice accretion occurs on the bottom of the bounding upper solid ice block,
152 resulting in an advancing ice front that moves downward with time. Importantly, the appearance of
153 downward motion is entirely the result of upward motion of water vapor and subsequent deposition on the
154 ice surface. Conservation of mass at the solid ice/humid air interface requires

155

$$156 \quad \gamma_v v_v = -\gamma_i v_f, \quad (3)$$

157

158 where γ_v is the water vapor density, v_v is the vapor diffusion velocity, γ_i is the density of ice, and v_f is the
159 downward velocity of the accumulating ice front. By tracking the accumulating ice front over time at the
160 upper solid ice boundary, either experimentally or theoretically, one is afforded the remarkable
161 opportunity to quantify the surface mass flux, $\gamma_v v_v$, transcending the upper boundary.

162

163 Similarly, the mass flux across the lower boundary is the amount of mass passing through the
164 lower bounding surface per unit of area per unit of time. Physically, it is the amount of ice in the lower
165 solid ice block sublimating to water vapor at the solid ice/humid air boundary. As time proceeds,
166 sublimation off the lower block results in a receding ice front on the lower bounding ice block that moves
167 downward with time. The rate of ice sublimation is also identical to the microscale humid air mass
168 flux, $\gamma_v v_v$.

169

170 The conclusion, then, is that the mass transfer moving through the layered ice/humid air system is
171 the same as the mass flux sublimating from the lower solid ice surface and depositing on the upper ice
172 surface and this mass flux is given by $\gamma_v v_v$. Finally, a bit of numerical context is useful here in that the
173 magnitude of (v_f / v_v) is on the order of 10^{-6} .

174

175 2.2 The energy flux of humid air as a pure substance

176

177 The energy flux of humid air as a pure substance follows the classic work on *Transport*
178 *Phenomena* by Bird et al. (1960). In brief, the total energy flux for humid air may be written as

179

$$180 \quad \mathbf{q} = \mathbf{q}^{(c)} + \mathbf{q}^{(d)} \quad (4)$$

181

182 where $\mathbf{q}^{(c)}$ is the conductive flux and $\mathbf{q}^{(d)}$ represents “contribution from the interdiffusion of the various
183 species present.” Utilizing Fourier’s law for the conductive flux and Fick’s law for the diffusive flux
184 (Bird et al., 1960), the 1D energy flux for humid air may be expressed as (Hansen and Foslien, 2015)

185

$$186 \quad q = -\left(k_{\text{ha}} + u_{\text{sg}} \left(\frac{d\gamma_v}{d\theta}\right) D_{v-a}\right) \frac{\partial\theta}{\partial x}, \quad (5)$$

187

188 where k_{ha} is the thermal conductivity, D_{v-a} is the binary diffusion coefficient of water vapor in air,
189 u_{sg} is the latent heat of sublimation of ice, and θ is the temperature. Following Bird et al. (1960) one
190 can identify

191

$$192 \quad \text{conductive flux} = -k_{\text{ha}} \frac{\partial\theta}{\partial x}, \quad (6)$$

193



194 and

195

$$196 \quad \text{mass flux} = \gamma_v u_v = -D_{v-a} \left(\frac{d\gamma_v}{d\theta} \right) \frac{\partial \theta}{\partial x} \quad (7)$$

197

198

199 **3. Comparing the diffusion coefficient definitions**

200

201 In order to model the thermophysical processes in a snowpack, knowledge of the macroscale
 202 energy flux for snow is required. The energy flux is given by

203

$$204 \quad q_s = - \left(k_s + u_{sg} \left(\frac{d\gamma_v}{d\theta} \right) D_s \right) \frac{\partial \theta}{\partial x} \quad (8)$$

205

206 where k_s is the thermal conductivity and D_s is the diffusion coefficient for snow. While these properties
 207 influence the temperature profile through the snowpack, they also evolve with the changing microstructure
 208 that occurs during snow metamorphism. As such, analytical models for each of these parameters are
 209 sought that can account for microstructural evolution, a lofty goal to be sure.

210

211 **3.1 The layered microstructure**

212 The exact macroscale energy flux density for the layered ice/humid air microstructure is fully
 213 developed in Hansen and Foslien (2015). However, a dramatic simplification of the analytical form of the
 214 energy flux may be achieved by restricting ice volume fractions to be less than 0.8. This simplified form
 215 of the energy flux is given by

$$216 \quad q_{lm} = - \left(\left(\frac{k_{ha}}{\phi_{ha}} \right) + \left(\frac{D_{v-a}}{\phi_{ha}} \right) u_{sg} \frac{d\gamma_v}{d\theta} \right) \frac{\partial \theta}{\partial x} \quad (9)$$

217

218 where the subscript “lm” denotes “layered microstructure.” Figure 4 provides a comparison of the exact
 219 energy flux and the approximate energy flux of Eq. (9) at -2°C . The figure shows the exact and
 220 approximate forms of the energy flux are nearly identical for $\phi_i < 0.8$. Furthermore, the approximate
 221 form is most accurate at low densities where diffusion is most prominent. Equation (9) serves as a starting
 222 point for the discussion of the two definitions of the diffusion coefficient.

223

224 An important feature of the development of the energy flux of the layered microstructure is that
 225 the energy flux of the macroscale continuum is identical to the energy flux of the ice and humid air
 226 constituents respectively, i.e.,

227

$$228 \quad q_{lm} = q_{ha} = q_i \quad (10)$$

229

230 This relationship is used repeatedly to transition from the macroscale to the humid air microscale

231

232 **3.2 The bounding surface flux approach to the diffusion coefficient**

233

234 The macroscale energy flux of Eq. (9) can be placed into a familiar form for heat transfer in
 235 humid air alone as presented in Section 2.2. By restricting the ice volume fraction to values below 0.8,
 236 the constituent temperature gradients may be approximated as

237

$$238 \quad \left(\frac{\partial \theta}{\partial \xi} \right)_i \approx 0 \quad \text{and} \quad \left(\frac{\partial \theta}{\partial \xi} \right)_{ha} = \left(\frac{1}{\phi_{ha}} \right) \frac{\partial \theta}{\partial x} \quad .$$

239
 240 Noting the above and recognizing the energy flux at the macroscale is identical to the energy flux through
 241 the humid air layer leads to

$$242 \quad 243 \quad q_{\text{lm}} = q_{\text{ha}} = - \left(k_{\text{ha}} + D_{\text{v-a}} u_{\text{sg}} \frac{d\gamma_{\text{v}}}{d\theta} \right) \left(\frac{\partial \theta}{\partial \xi} \right)_{\text{ha}} . \quad (11)$$

244
 245 Equation (11) is recognized as a precise restatement of Eqs. (4) and (5), defining the energy flux of
 246 humid air as a pure substance following the classic work on *Transport Phenomena* by Bird et al. (1960)—
 247 a fundamental ground truth. Following Bird et al. one can write

$$248 \quad 249 \quad \text{conductive flux} = -k_{\text{ha}} \left(\frac{\partial \theta}{\partial \xi} \right)_{\text{ha}} \\ 250 \quad 251 \quad = - \left(\frac{k_{\text{ha}}}{\phi_{\text{ha}}} \right) \frac{\partial \theta}{\partial x} , \quad (12)$$

252 and

$$253 \quad 254 \quad \text{mass flux} = -D_{\text{v-a}} \left(\frac{d\gamma_{\text{v}}}{d\theta} \right) \left(\frac{\partial \theta}{\partial \xi} \right)_{\text{ha}} \\ 255 \quad 256 \quad = - \left(\frac{D_{\text{v-a}}}{\phi_{\text{ha}}} \right) \left(\frac{d\gamma_{\text{v}}}{d\theta} \right) \frac{\partial \theta}{\partial x} . \quad (13)$$

258 Note that the conductive flux and the mass flux identified above are correct for the macroscale
 259 layered continuum as well as the microscale of the pure humid air layer. Specifically, the mass flux of Eq.
 260 (13) is identical to the surface flux of water vapor crossing the boundaries at the interface of the solid
 261 ice/humid air mixture—at the upper boundary in the form of deposition and ice accretion as well as at the
 262 lower boundary in the form of sublimation. In other words, Eq. (13) represents the mass flux moving
 263 through the ice/humid air mixture.

264 Consistent with the above discussion, the conductive heat flux and mass flux lead to following
 265 definitions of thermal conductivity and the diffusion coefficient given by

$$266 \quad 267 \quad 268 \quad k_{\text{lm}} = \left(\frac{k_{\text{ha}}}{\phi_{\text{ha}}} \right) . \quad (14)$$

269 and

$$270 \quad 271 \quad 272 \quad D_{\text{lm}} = \left(\frac{D_{\text{v-a}}}{\phi_{\text{ha}}} \right) . \quad (15)$$

273 While the specific forms of the conductive flux and mass flux given in Eqs. (12) and (13) may
 274 seem intuitively obvious for a layered ice/humid air microstructure and further represent a ground truth
 275 for energy transfer in humid air as a pure substance, they are at the very heart of the historical (and
 276 current) controversy surrounding the diffusion coefficient.

277
 278
 279 Forteau et al. (2021a) argue that the decomposition of Eq. (9) into a conductive flux and a mass
 280 flux defined by Eqs. (12) and (13) is not unique and other decompositions exist. In particular, their
 281 arguments focus on volume averaging the local (microscale) mass flux to obtain the macroscale mass
 282 flux.



283

284

3.3 A volume averaged approach to the diffusion coefficient

285

286

287

288

289

290

291

$$D_{\text{lm}} = D_{v-a} \quad (16)$$

292

293

294

Noting the energy flux of Eq. (9), the above definition of the diffusion coefficient leads to a definition of thermal conductivity given by (see Eq. C7, Appendix C, Fourteau et al., 2021a)

295

$$k_{\text{lm}} = \left(\frac{k_{\text{ha}} + \phi_i D_{v-a} u_{\text{sg}} \left(\frac{dy_v}{d\theta} \right)}{\phi_{\text{ha}}} \right) \quad (17)$$

296

297

298

The above thermal conductivity and diffusion coefficient decomposition suggested by Fourteau et al. (2021a, 2021b), while a correct mathematical decomposition of the energy flux, has some troubling aspects related to the physics of heat and mass transfer in the layered microstructure including:

299

300

301

302

303

304

305

306

307

308

309

310

- The diffusion coefficient of Eq. (16) does not predict the known mass transport of water vapor leaving the upper boundary of Figure 2(a) in the form of ice accretion on the upper solid ice block, or water vapor crossing the lower boundary in the form of sublimation from the lower ice block. Moreover, it clearly does not represent the total mass transfer due to diffusion as the thermal conductivity of Eq. (17) also contains a diffusion term.
- The thermal conductivity of Eq. (17) does not represent a true thermal conductivity for the layered microstructure, which is correctly defined by Eq. (14). Equation (14) is simply a statement of ground truth for thermal conductivity of humid air as a pure substance as outlined in Section 2.2. In brief, why should the thermal conductivity of humid air as a pure substance involve diffusion.

311

312

313

314

315

316

The lack of physical meaning of the conductive flux and the mass flux of the approach of Fourteau et al. (2021a, b) may be traced to their definition of the diffusion coefficient based on a volume average of the local (microscale) diffusion velocity. A precise explanation as to why the volume averaging of the mass flux put forth by Fourteau (2021a) fails to model the mass flux across the boundaries is provided in Section 4.3.

317

318

3.4 The role of hand-to-hand water vapor transport in the macroscale heat and mass transport properties

319

320

321

322

Sections 3.2 and 3.3 lay out two separate views of mass diffusion occurring in a layered ice/humid air microstructure. In what follows, additional physical insight into the connection and fundamental differences of the two approaches is provided. In doing so, the role of hand-to-hand water vapor transport in mass diffusion is revealed.

323

324

Again, begin with the normalized energy flux of the layered microstructure taken from Eq. (9) and written as



$$325 \quad \frac{q}{\left(\frac{\partial \theta}{\partial x}\right)} = - \left(\frac{k_{ha}}{\phi_{ha}} + \left(\frac{D_{v-a}}{\phi_{ha}}\right) u_{sg} \left(\frac{d \gamma_v}{d \theta}\right) \right). \quad (18)$$

326 The second term on the RHS of the above involving diffusion may be broken out into two terms
 327 weighted by volume fractions of ice and humid air leading to

$$328 \quad \frac{q}{\left(\frac{\partial \theta}{\partial x}\right)} = - \left(\underbrace{\frac{k_{ha}}{\phi_{ha}}}_{(1)} + \underbrace{\phi_i \left(\frac{D_{v-a}}{\phi_{ha}}\right) u_{sg} \left(\frac{d \gamma_v}{d \theta}\right)}_{(2)} + \underbrace{\phi_{ha} \left(\frac{D_{v-a}}{\phi_{ha}}\right) u_{sg} \left(\frac{d \gamma_v}{d \theta}\right)}_{(3)} \right). \quad (19)$$

330 The approach of Fourteau et al. (2021a) presented in Section 3.3 combines Terms 1 and 2 of Eq.
 331 (19) to arrive at thermal conductivity and diffusion coefficient definitions given by

$$332 \quad k_{lm} = \left(\frac{k_{ha}}{\phi_{ha}}\right) + \phi_i \left(\frac{D_{v-a}}{\phi_{ha}}\right) u_{sg} \left(\frac{d \gamma_v}{d \theta}\right), \quad (20)$$

333 and

$$334 \quad D_{lm} = D_{v-a}. \quad (21)$$

335 As a general observation, Terms 2 and 3 of Eq. (19) clearly involve mass transfer involving the
 336 diffusion coefficient of water vapor in air. As noted previously, logic would suggest that these terms be
 337 grouped together, rather than combining a mass diffusion term with thermal conductivity as done in Eq.
 338 (20).

339 In contrast, the approach of grouping the similar diffusion terms, Term 2 & 3 of Eq. (19), is
 340 followed in Section 3.2, leading to the thermal conductivity and diffusion coefficient having the
 341 definitions of

$$342 \quad k_{lm} = \left(\frac{k_{ha}}{\phi_{ha}}\right), \quad (22)$$

343 and

$$344 \quad D_{lm} = \left(\frac{D_{v-a}}{\phi_{ha}}\right). \quad (23)$$

345 The above definitions are developed from a macroscale energy flux of Eq. (9) that is identical to
 346 the energy flux of humid air as a pure substance at the microscale. Equation (23), and its associated mass
 347 flux given by Eq. (13) also represents the true mass transfer across the upper and lower boundaries of
 348 Figure 2(a). Finally, note the striking similarities in Eqs. (22) and (23) and their elegant simplicity.

349 The differences in the approaches of Sections 3.2 and 3.3 clearly fall to the second term of Eq.
 350 (19). The fundamental question, then, is “what is the precise physical significance of the second term?”
 351 The answer is that this term is the mass diffusion and heat transfer associated with hand-to-hand analogy
 352 of water vapor transport involving the simultaneous condensation and sublimation of water vapor in the
 353 ice phase. To show this physically, note that the volume fractions of ice and humid air are identical to the



354 lineal fraction for a test line of length, L , passing through the microstructure. Hence Terms 2 and 3 in Eq.
355 (19) may be combined to show the heat flux due to mass diffusion is

356
$$\text{diffusion heat flux} = - \left[\frac{L_i}{L} \left(\frac{D_{v-a}}{\phi_{ha}} \right) u_{sg} \left(\frac{d\gamma_v}{d\theta} \right) + \frac{L_{ha}}{L} \left(\frac{D_{v-a}}{\phi_{ha}} \right) u_{sg} \left(\frac{d\gamma_v}{d\theta} \right) \right] \frac{\partial \theta}{\partial x}, \quad (24)$$

357 where L_i and L_{ha} are the respective lengths of a test line passing through the ice phase and the humid air
358 phase. The associated mass flux is given by

359
$$\text{mass flux} = - \left(\underbrace{\frac{L_i}{L} \left(\frac{D_{v-a}}{\phi_{ha}} \right)}_{(A)} + \underbrace{\frac{L_{ha}}{L} \left(\frac{D_{v-a}}{\phi_{ha}} \right)}_{(B)} \right) \left(\frac{d\gamma_v}{d\theta} \right) \frac{\partial \theta}{\partial x} \quad (25)$$

360

361 Term B in Eq. (25) represents the mass flux due to water vapor diffusion through the humid air
362 scaled by the normalized length of a humid air test line. It is this term that Fourteau et al. (2021a) have
363 identified as the diffusive mass flux for the macroscale layered microstructure.

364 Term A in Eq. (25) may be viewed as the mass flux from hand-to-hand water vapor transport by
365 the ice phase as a result of continuous condensation and sublimation. Physically, with regard to hand-to-
366 hand water vapor transport, the ice phase can only transfer mass as fast as it receives it from the humid air
367 and this is precisely governed by the humid air mass flux at the microscale given by

368
$$\gamma_v v_v = \left(\frac{D_{v-a}}{\phi_{ha}} \right) \left(\frac{d\gamma_v}{d\theta} \right) \frac{\partial \theta}{\partial x}. \quad (26)$$

369 The above result is then scaled by the ice lineal ice fraction (L_i/L) for the layered microstructure
370 to account for the distance covered by the ice phase as vapor hop scotches across the ice phase. As soon
371 as vapor arrives at a lower ice surface, an equivalent amount leaves the upper surface. The end result is
372 precisely Term A in Eq. (25).

373 While the above discussion provides a cogent physical explanation of the role of hand-to-hand
374 vapor transport in the diffusion coefficient, one may argue that the discussion lacks the necessary
375 mathematical rigor to be wholly defensible. This weakness is dispelled in Sections 4 & 5 through a
376 rigorous control volume analysis, as well as tracking a material point of water throughout its life in
377 traveling through the microstructure to the upper solid ice boundary.

378
379

380 4. Control volume analysis

381

382 The continuum forms of the governing balance equations of mass, momentum, and energy are
383 developed in terms of a material volume—a region in space containing a known quantity of mass. As the
384 body is deformed, the material volume moves in space and may also deform in shape. Moreover, in the
385 case of fluids, the configuration of the deformed body is generally not known until the problem is solved.

386 To alleviate the challenges of studying a material volume, the idea of a control volume is
387 introduced where one defines a region in space to apply the governing equations. Sonin (2003) provides
388 an excellent discussion of control volumes stating: “A control volume is an arbitrarily defined volume
389 with a closed bounding surface (the control surface) that separates the universe into two parts: the part
390 contained within the control volume, and the rest of the universe. The control surface is a mental
391 construct, transparent to all material motion, and may be static in the chosen reference frame, or moving



392 *and expanding or contracting in any specified manner. The analyst specifies the velocity $v(r,t)$ at all*
393 *points of the control surface for all time.”* The selection of a control volume is driven by the information
394 that is desired.

395 In this section, two control volume analyses are presented for the layered ice/humid air
396 microstructure, including a fixed control volume and a moving control volume that moves downward in
397 lockstep with the downward advancing ice front on the top boundary, see Figure 5. For brevity, in the
398 following discussion, the upper and lower ice blocks are referred to as “solid ice” while the layered
399 ice/humid air microstructure is simply referred to as the “ice mixture.”

400
401 Let the fixed control volume and the moving control volume be coincident at time $t = 0$ as
402 shown in Figure 5(a). At a later time, the moving control volume has diverged from the fixed control
403 volume as it tracks the moving ice front formed by ice accretion at the upper boundary, Figure 5(b). Note
404 that, as $t \rightarrow \infty$, the ice phase would advance sufficiently such that the entire fixed control volume would
405 enclose ice only.

406 407 **4.1 Mass flux of humid air as a pure substance**

408
409 The mass flux of humid air as a pure substance provides an important foundation for
410 understanding the mass flux of the layered microstructure. Figure 6(a) shows the advancing ice front from
411 the upper boundary due to ice accretion from water vapor transport due to diffusion in humid air alone.
412 Now introduce a characteristic time, τ , at which the advancing ice front at the upper boundary has moved
413 a length, ℓ . The total mass contained in the advancing ice front may be expressed in several forms given
414 by:

$$415 \gamma_v \hat{v}_v \tau = -\gamma_i \hat{v}_f \tau = \gamma_i \ell \quad , \quad (27)$$

416
417 where the hats above the velocity symbols are used to refer to humid air as a pure substance. The
418 characteristic time and length (τ , ℓ) for humid air as a pure substance serve as a valuable baseline for the
419 analysis of the layered microstructure.

420
421 A subtle but important observation throughout the analysis of this section is that the true water
422 vapor diffusion velocity is unaffected by the speed of the advancing ice front as (\hat{v}_f / \hat{v}_v) is on the order
423 of 10^{-6} .

424
425 Fluid mechanics is replete with solutions involving moving control volumes and these moving
426 control volumes often track the motion of a moving front. In the present case, the moving control volume
427 tracks the advancing ice front at the upper boundary and the receding ice front at the lower boundary, (the
428 green control volume of Figure 5(b)). The following fundamental properties of the analysis are observed
429 for humid air as a pure substance:

430
431
432 1) The mass of the control volume is constant in time implying

$$433 \frac{d}{dt} \int_{\mathcal{R}} \rho dV = 0 \quad . \quad (28)$$

434
435 The Reynold’s Transport Theorem for mass conservation may be expressed in the form
436 (Sonin, 2003)

$$437 \frac{d}{dt} \int_{\mathcal{R}(t)} \rho dV + \int_{\partial \mathcal{R}(t)} \rho (\hat{v}_v - v_C) dV = 0 \quad , \quad (29)$$



440 where v_C is the control surface velocity. Recognizing $v_C = v_f$, the transport theorem for
 441 water vapor reduces to
 442

443
 444
$$\int_{\partial\mathcal{R}(t)} \gamma_v (\hat{v}_v - v_f) dV = 0 . \quad (30)$$

445
 446 Noting (v_f / \hat{v}_v) is on the order of 10^{-6} , there follows
 447

448
$$\int_{\partial\mathcal{R}(t)} \gamma_v \hat{v}_v dV = 0 . \quad (31)$$

449 The above simply implies the mass of water vapor entering the control volume from below is
 450 equal to the mass of water vapor leaving the control volume from above.
 451

452 2) The control volume boundaries continuously lie at the interface between the solid ice and the
 453 ice mixture. Hence, mass transfer across the control volume surface is precisely the mass flux
 454 of water vapor crossing the boundaries between the humid air and the bounding solid ice. The
 455 mass flux across the upper and lower boundaries is governed by
 456

457
 458
$$\text{mass flux} = \gamma_v \hat{v}_v = D_{v-a} \left(\frac{d\gamma_v}{d\theta} \right) \frac{\partial\theta}{\partial x} . \quad (32)$$

459 Sublimation is occurring at the lower boundary while deposition of water vapor is occurring
 460 at the upper boundary.
 461

462
 463 **4.2 Layered microstructure: moving control volume**
 464

465 As in the case of humid air as a pure substance, let the moving control volume track the moving
 466 ice front at the boundaries. The following fundamental properties of the analysis are observed:
 467

468 1) The mass of the control volume is constant in time implying yielding Eq. (28). Following
 469 identical arguments to those for humid air as a pure substance, the mass flux across the
 470 control surface may be written as
 471

472
$$\int_{\partial\mathcal{R}(t)} \gamma_v v_v dV = 0 , \quad (33)$$

473 implying the mass of water vapor entering the control volume from below is equal to the
 474 mass of water vapor leaving the control volume from above.
 475

476
 477 2) The control volume boundaries continuously lie at the interface between the solid ice and the
 478 ice mixture. Hence, mass transfer across the control volume surface is precisely the mass flux
 479 of water vapor transcending the boundaries between the ice mixture and the bounding solid
 480 ice. The mass flux across the upper and lower boundaries is enhanced due to the elevated
 481 humid air temperature gradient and is governed by Eq. (13) as
 482

483
$$\text{mass flux} = \gamma_v v_v = \left(\frac{D_{v-a}}{\phi_{ha}} \right) \left(\frac{d\gamma_v}{d\theta} \right) \frac{\partial\theta}{\partial x} . \quad (34)$$

484 Comparing Eqs. (32 & 34) one can write
 485

486
 487
$$\gamma_v v_v = \frac{\gamma_v \hat{v}_v}{\phi_{ha}} . \quad (35)$$



488
 489 A comparison of the mass flux for the layered microstructure versus the mass flux of humid air
 490 alone is most readily followed through a choice of specific constituent volume fractions. Hence, consider
 491 an ice volume fraction of $\phi_i = 1/3$, implying $\phi_{ha} = 2/3$. For this case, the mass flux of the layered
 492 microstructure given in Eq. (35) is 1.5 times the mass flux of humid air as a pure substance. Furthermore,
 493 for the characteristic time, τ , the ice front advancing from the upper boundary has moved 1.5ℓ compared
 494 to ℓ for humid air as a pure substance, Figure 6(b).
 495

496 Now consider a unit cell for a *moving control volume* advancing with the ice front shown in
 497 Figure 7(a). Further, define a local coordinate system (ξ) moving downward with the control volume.
 498 Hence, the coordinate system is moving downward at the speed of the accumulating ice front on the lower
 499 boundary of the unit cell. Two interesting observations fall out:
 500

- 501 • The problem is steady state relative to the moving reference frame meaning the configuration of
 502 the unit cell is unchanged with time. Hence, the mass within the control volume is time
 503 independent, as is the surface flux across the boundaries of the unit cell.
 504
- 505 • Relative to an observer on the control volume, *an arbitrary material point in the ice phase is*
 506 *seen moving upwards toward the upper surface of the ice* with a velocity of $v_{i/C} = -v_f$, where
 507 $v_{i/C}$ is the velocity of material point with respect to the control volume.
 508

509 A mass balance at the solid vapor interface in the unit cell yields

$$510 \quad \gamma_i v_{i/C} = -\gamma_i v_f = \gamma_v v_v \quad (36)$$

511 The mass flux across the upper and lower boundaries of the unit cell is given by

$$512 \quad \text{mass flux} = \gamma_v v_v = \left(\frac{D_{v-a}}{\phi_{ha}}\right) \left(\frac{d\gamma_v}{d\theta}\right) \frac{\partial\theta}{\partial x} \quad (37)$$

513 The volume average of the mass flux over the entire volume of the unit cell is given by

$$514 \quad \text{mass flux} = \phi_{ha} \gamma_v v_v + \phi_i \gamma_i v_{i/C} \\ 515 \quad = (\phi_{ha} + \phi_i) \gamma_v v_v = \gamma_v v_v = \left(\frac{D_{v-a}}{\phi_{ha}}\right) \left(\frac{d\gamma_v}{d\theta}\right) \frac{\partial\theta}{\partial x} \quad (38)$$

516 Importantly, the volume averaged mass flux and the surface mass flux agree. Furthermore, the
 517 term $\phi_i \gamma_i v_{i/C} = \phi_i \gamma_v v_v$ in Eq. (38) is numerically equal to the hop scotching effect of hand-to-hand
 518 vapor transport described in Section 3.4.
 519

520 An additional appealing aspect of this moving control volume analysis is that the configuration of
 521 the unit cell does not matter. For instance, consider the unit cell of Figure 7(b) where the unit cell
 522 boundaries extend through the ice phase. Equations (36-38) remain valid and the configuration of the unit
 523 cell remains steady-state (time independent).
 524

525 ***Perhaps the most important aspect of the unit cell analysis of the moving control volume is that***
 526 ***the ice phase is a contributing factor to the overall mass transport of water moving through the system.***
 527 As a result, diffusion of water vapor is enhanced at all humid air volume fractions. This result is at odds
 528



535 with the authors who suggest the only role of the ice phase is to occupy volume where diffusion cannot
536 occur, an untenable position regarding mass transfer in the layered microstructure.

537

538 **4.3 Layered microstructure: fixed control volume**

539

540 Now consider the mass transfer analysis of the layered microstructure using a fixed control
541 volume shown by the red dashed line in Figure 5(b)—a decidedly more complicated approach. Note that
542 the advancing ice front moves downward into the control volume due to ice accretion on the solid ice/ice
543 mixture boundary. The mass flux at the upper solid ice/ice mixture boundary is governed by Eq. (34).

544

545 Before discussing mass transfer through the lower boundary of the control volume, let us examine
546 a unit cell in the context of a fixed control volume. Figure 8(a) shows a unit cell at time $t = 0$. As time
547 proceeds, the ice phase advances downward due to condensation and sublimation on the upper and lower
548 ice boundaries, respectively. Figure 8(b) shows this downward advancing ice mass at a later time.
549 Eventually the ice mass will pass through the lower boundary as it simultaneously reappears at the upper
550 boundary.

551

552 Three important observations governing mass transfer in the fixed control volume unit cell are:

553

554 • While the ice phase *appears* to be propagating downward, it is caused by water vapor
555 moving upward with a monotonically increasing (nonnegative) displacement. *All* material
556 points of water in the system are either diffusing upward through the humid air or at zero
557 velocity while locked in the ice phase. Water material points never have a negative
558 velocity, despite the ice phase *appearance* of downward motion.

559

560 • The volume average of the humid air mass flux within the unit cell is given by

561

$$562 \langle \gamma_v v_v \rangle = D_{v-a} \left(\frac{d\gamma_v}{d\theta} \right) \frac{\partial \theta}{\partial x}. \quad (39)$$

563

564 • The surface flux across control volume boundaries is non-steady but periodic. In other
565 words, at times the ice phase will block vapor transport across a control volume
566 boundary while at other times vapor will pass through a humid air boundary of the
567 control volume. A temporal average over one period of the surface flux over either the
568 upper or lower boundaries reveals a flux identical to the volume average given by

569

$$570 \overline{\gamma_v v_v} = D_{v-a} \left(\frac{d\gamma_v}{d\theta} \right) \frac{\partial \theta}{\partial x}. \quad (40)$$

571

572 Hence, the time averaged surface flux over the upper and lower boundaries of the unit cell agrees with
573 volume averaged mass flux.

574

575 One is now faced with an interesting paradox that strikes at the heart of the debate over the
576 definition of the diffusion coefficient. One can summarize the conflict with the following observations
577 made for the fixed control volume of Figure 5(b):

578

579 • The rate of mass transfer in the form of ice accretion at the solid ice/ice mixture upper
580 boundary is given by Eq. (34) as:

581

$$582 \gamma_v v_v = \frac{\gamma_v \hat{v}_v}{\phi_{ha}} = \frac{D_{v-a}}{\phi_{ha}} \left(\frac{d\gamma_v}{d\theta} \right) \frac{\partial \theta}{\partial x}$$

583



584 • The volume average microscale mass flux is given by Eq. (39) as

585

$$586 \quad \langle \gamma_v v_v \rangle = \gamma_v \hat{v}_v = D_{v-a} \left(\frac{d\gamma_v}{d\theta} \right) \frac{\partial \theta}{\partial x}.$$

587

588 • The temporal average flux across the lower boundary of the fixed control volume is given
589 by Eq. (40), i.e.

590

$$591 \quad \overline{\gamma_v v_v} = \gamma_v \hat{v}_v = D_{v-a} \left(\frac{d\gamma_v}{d\theta} \right) \frac{\partial \theta}{\partial x}$$

592

593 *An apparent conflict arises in that the mass flux crossing the upper solid ice/ice mixture*
594 *boundary exceeds the mass flux entering the control volume from the lower surface which is also equal to*
595 *the volume average of the microscale mass flux.*

596

597 The conflict is resolved through a careful examination of the role of the ice phase that exists in
598 the form of layering within the fixed control volume. Specifically, individual layers of ice act as large
599 reservoirs that release water vapor as needed, allowing the water vapor to diffuse through the humid air.

600

601 Consider a fixed control volume as shown in Figure 9(a). The reservoirs of water vapor contained
602 in the ice layers in the control volume disappear over time as they effectively restore the mass imbalance
603 across the control volume boundaries described above. For example, suppose at time $t = 0$, there are 50
604 layers of ice within the fixed control volume of Figure 9(a). At a later time, as the ice front advances
605 downward from the solid ice upper boundary, there may only be 40 layers. At still a later time, 30 layers
606 will exist and so on. Eventually, all layers of ice will have vanished through diffusion in the humid air,
607 arriving at the upper solid ice boundary in the form of ice accretion. In brief, the ice phase is definitely
608 contributing to the mass transfer through the layered microstructure. In fact, the ice phase is a major
609 source of water vapor while the humid air acts as the transport mechanism.

610

611 The opposite phenomenon is occurring in the fixed control volume of Figure 9(b). Here,
612 sublimation at the lower solid ice/ice mixture boundary has a mass flux entering the layered
613 microstructure at the rate of Eq. (34). The mass flux leaving the upper boundary is defined by the surface
614 flux of Eq. (40), also equal to the humid air mass flux volume average of Eq. (39). *An apparent conflict*
615 *again arises in that the mass flux crossing the lower solid ice/ice mixture boundary exceeds the mass flux*
616 *leaving the control volume from the upper surface of Figure 9(b).*

617

618 The conflict is again resolved by the presence of the ice layering. Whereas, in the control volume
619 of Figure 9(a) where ice layers disappear over time, in the control volume of Figure 9(b), ice layers grow
620 in number over time. For example, suppose at time $t = 0$, there are 50 layers of ice within the fixed
621 control volume of Figure 9(b). At a later time, as the solid ice recedes at the lower boundary, the number
622 of layers may rise to 60 layers. At still a later time, 70 layers will exist and so on. Note that the total
623 number of layers in the entire system, defined as the sum of layers in Figure 9(a) and 9(b) is constant as
624 the problem is steady state.

625

626 Just like the analysis of the moving control volume, in the case of the fixed control volume
627 analysis, ***the ice phase is a major contributing factor to the overall mass transport of water moving***
628 ***through the system.*** This “reservoir phenomenon” explains why the simple volume averaging of the
629 humid air microscale mass flux proposed by Fourteau et al. (2021) does not correctly capture the mass
630 flux of water “moving” through the system.

631



632 As a numerical example of the ice reservoir effect, consider an ice volume fraction of $\phi_i = 1/3$,
633 implying $\phi_{ha} = 2/3$. Further, assume the control volume has length $1.5 L$ such that an advancing ice
634 front will fill the control volume in time τ , Figure 9(a). At time $t = 0$, the ice phase present in the mixture
635 in the form of layering has a total mass of

$$636 \quad \phi_i \gamma_i 1.5\ell = 0.5\gamma_i \ell \quad (41)$$

637
638 As noted previously, the appearance of individual ice layers moving in a downward direction
639 causing a counterflux of mass is a mirage, as water (ice or vapor) is always moving upward in a
640 monotonically increasing (nonnegative) fashion. In particular, water vapor is either advancing toward the
641 upper boundary in the form of diffusion through the humid air or stationary as solid ice, waiting to reach
642 the surface of a layer to take off again. The implication of this observation is that all mass within the ice
643 layers of the control volume at $t = 0$ will reach and become part of the advancing ice front at the solid
644 ice/ice mixture boundary.
645

646
647 At the same time that the ice layers within the control volume are contributing to the mass flux
648 over time τ , additional mass enters the fixed control volume from below according to Eq. (39) at the time
649 averaged rate of $\gamma_v \hat{v}_v$, identical to the mass flux of humid air as pure substance. From Eq. (27) of Section
650 4.1, the mass added to the fixed control volume by crossing the lower boundary in time τ is

$$651 \quad \gamma_v \hat{v}_v \tau = -\gamma_i \hat{v}_f \tau = \gamma_i \ell \quad (42)$$

652
653 The total mass of the advancing front at the solid ice/ice mixture boundary is the sum of Eqs. (41) and
654 (42) given by $\gamma_i 1.5\ell$, making the control volume solid of Figure 9(a) solid ice.
655
656

657 In brief, mass added across the fixed control volume lower surface plus additional ice mass
658 present in the control volume in the form of ice reservoirs equals the total mass of ice of the advancing ice
659 front. *Or, in terms of diffusion, the mass flux attributed to the layered ice within the fixed control volume*
660 *plus the mass flux crossing the lower boundary of the fixed control volume equals the total mass flux*
661 *across the upper solid ice/ice mixture boundary.* In brief, the layered ice within the control volume should
662 be viewed as a reservoir of water vapor that enhances diffusion rather than a temporal storage of water
663 vapor slowing diffusion.
664

665 The complexities of the fixed control volume are subtle and require attention to detail. Of course,
666 all of these complexities can be dispensed with by formulating the mass transfer problem in terms of a
667 moving control volume as was done in Section 4.2. In either the case of the moving control volume or the
668 fixed control volume, the mass transfer across the solid ice/ice mixture boundary is identical—physics
669 demands a solution that is independent of the control volume selected. Furthermore, water vapor diffusion
670 is enhanced at all ice volume fractions compared to diffusion through humid air as a pure substance. The
671 diffusion enhancement is identical to the results predicted by the hand-to-hand diffusion analogy put forth
672 by Yosida (1955).
673
674

675 5. The ice phase as a reservoir of water vapor

676
677 A fresh look at the diffusion problem allows one to dispense with hand-to-hand water vapor
678 transport as a diffusion mechanism. Figure 10 demonstrates the motion of two water vapor material
679 points, A and B , over a period of time sufficient for an ice layer to completely turn over its entire mass.
680 The linear upward sloping portion of the water vapor displacement of A and B represents time traveling
681 through humid air whereas the long constant period (zero velocity) represents time residing in the ice
682 phase. The water vapor transport cycle through a unit cell is complete at $t = t'$ when the water material



683 points are located at A' and B' and the cycle then repeats. Note that the concept of a counterflux of mass is
684 a myth in that the motion of water material points A and B is a monotonically increasing function for all
685 time.

686

687 Figure 10 also shows that as point A arrives at the bottom of the ice at A' , point B is ready to take
688 off through humid air at B' , just as occurred at $t = 0$. This phenomenon is precisely a description of hand-
689 to-hand vapor transport.

690

691 An alternative view of hand-to-hand diffusion is presented through a careful extrapolation of the
692 displacement/time history of Figure 10. If one tracks a single material point, A , it is clear that all vertical
693 motion of the point occurs as water vapor diffusing upward through humid air. This observation is, in
694 some sense, consistent with Fourteau et al. (2021a) suggesting diffusion is controlled by the microscale
695 diffusion within humid air. Furthermore, the notion that hand-to-hand water vapor transport is
696 nonphysical in the context of diffusion is removed, i.e., the path of point A —in moving from its location
697 at $t = 0$ to the upper boundary—never involves hand-to-hand water vapor transport.

698

699 The reservoir phenomenon is on brilliant display when one examines a moving control volume
700 described in Section 4.2. In this case, a beautiful analogy of the role of the ice is that of a lake with a
701 single inlet at one end and a single outlet at the other. Under steady state conditions, the inflow and
702 outflow to the lake have identical mass flow rates. If one adopts the hand-to-hand model of mass
703 transport, the lake acts as an instantaneous source/sink for the mass flow rate, just as the ice does in the
704 layered microstructure.

705

706 One can also avoid the hand-to-hand concept of mass transfer in the lake by recognizing the
707 effective 1D mass flow rate through the lake is identical to the inlet and outlet mass flow rates. While the
708 velocity within the lake is extremely low, the massive volume of water moving, albeit extremely slowly,
709 produces the same mass flow rate. In the case of mass transfer through the layered microstructure the
710 *velocity of ice with respect to the moving control volume* is an identical effect.

711

712 The fundamental difference in the two approaches to diffusion described in this paper then, is
713 that, rather than looking at the ice as blocking microscale diffusion, the ice phase should be viewed as an
714 existing reservoir of water vapor. If one returns to the path of material point A , the extended time spent in
715 the ice should not be seen as slowing diffusion, rather, point A resides in the reservoir of ice until needed,
716 when it reaches the upper surface through sublimation of the ice above it. Once point A reaches the upper
717 surface of a layer, it then sublimates and moves upward through classic diffusion in humid air until it
718 reaches the next layer (reservoir). Also, because of elevated temperature gradients in the humid air
719 layered microstructure, water vapor released from the ice travels through the humid air at an enhanced
720 diffusion velocity compared to the velocity through humid air as a pure substance.

721

722

5.1 A specific example of the reservoir effect

723 Let us briefly address the physical arguments put forth in Section 2 of Fourteau et al. (2021a)
724 regarding diffusion in a layered microstructure. To begin, we focus on the red and orange molecules of
725 Figure 1 of Fourteau et al. (2021a). In reference to the hand-to-hand mass transfer analogy they note:
726 “*For this mechanism to explain the experimental observations, the continuous deposition and sublimation*
727 *should produce a real mass flux from one can to the other, as if the depositing molecule reappeared as*
728 *the sublimating one. However, what actually happens is that the depositing molecule (represented as an*
729 *orange dot in Fig. 1) remains incorporated at the bottom of the ice grain, thus remaining in the first can.”*

730 This statement is not true for, if one tracks the motion of the orange molecule over time, the water vapor
731 molecule remains stationary within the ice until it reaches the surface through sublimation of the ice
732 above it. At that point, the orange vapor molecule is released via sublimation and allowed to again



733 transfer upward, de facto moving from the lower can to the upper can—the classic form of diffusion of
734 water vapor.

735 In what follows, we present a specific calculation to show that the path of a material point of
736 water through the layered microstructure of Figure 11 results in enhanced diffusion compared to diffusion
737 through humid air alone—a nonintuitive result.

738

739 Consider the diffusion life of the orange material point shown at point F in Figure 11 and the time
740 history taken to reach the upper solid ice/ice mixture interface. Let the unit cell have a length dimension
741 of one as a matter of convenience as the volume fractions then correlate to lengths, i.e.,

742

$$743 \quad L_{\alpha} = \phi_{\alpha} . \quad (43)$$

744

745 The total distance point F must move to reach the upper surface is given by ($2 L_{\text{ha}}$). Note that the
746 distance through the ice phase does not enter this calculation because, as the ice phase of the layer
747 sublimates away, ice is also condensing on the solid ice/ice mixture interface at the same rate.

748

749 The total time for the water material point at F to reach the upper surface of the solid ice/ice
750 mixture is the time required to traverse through the humid air plus the time while at rest and locked in the
751 ice phase. The humid air diffusion time is given by

752

$$753 \quad t_{\text{ha}} = \frac{(2 L_{\text{ha}})}{v_v} . \quad (44)$$

754

755 Recall that the diffusion velocity is elevated due to the elevated temperature gradient in the humid air of
756 the layered microstructure and may be computed using Eq. (26).

757

758 To compute the total time the material point F resides in the ice phase, one must compute the
759 time it takes for the sublimating ice at the top of the layer to reach point F , currently residing at the
760 bottom of the ice layer. From Eq. (36), conservation of mass at the upper ice/humid air interface of the
761 ice layer leads to

762

$$763 \quad -\gamma_i v_f = \gamma_v v_v , \quad (45)$$

764

765 where v_f is the velocity of the receding front of the upper surface of the ice layer. The total time that the
766 point F resides locked in the ice phase is given by

767

$$768 \quad t_i = \frac{-L_i}{v_f} = \frac{(L_i)}{v_v} \left(\frac{\gamma_i}{\gamma_v} \right) \quad (46)$$

769

770 The total time for the material point at F to reach the upper solid ice/ice mixture surface is then

771

$$772 \quad \tau = t_{\text{ha}} + t_i$$

773

$$774 \quad = \frac{(2 L_{\text{ha}})}{v_v} + \frac{(L_i)}{v_v} \left(\frac{\gamma_i}{\gamma_v} \right) \quad (47)$$

775

776 When point F reaches the solid ice/ice mixture interface, thereby ending its travels, the amount of
777 mass per unit area reaching the upper surface in the form of deposited ice is given by

778

$$779 \quad m = \gamma_v (2 L_{\text{ha}}) + \gamma_i L_i . \quad (48)$$

780



781 Now consider humid air only under the same macroscale temperature gradient as the layered
 782 microstructure, Figure 6(a). One can compare the mass transfer rates between humid air alone and the
 783 layered microstructure in two different ways: i) compute the time required to achieve the same transfer of
 784 mass, or ii) fix the time and compute the quantity of mass that reaches the solid ice/ice mixture boundary
 785 in the form of deposition.

786
 787 Let us begin by fixing the mass according to Eq. (48) and compute the time required to achieve
 788 this mass transfer for humid air alone. To begin, the length, d , of a column of humid air needed to achieve
 789 the total mass of Eq. (48) is given by

790
 791
$$d = \frac{m}{\gamma_v} = (2 L_{ha}) + \left(\frac{\gamma_i}{\gamma_v}\right) L_i \quad . \quad (49)$$

792
 793 As noted previously, the diffusion velocity is elevated in the humid air/ice mixture compared to
 794 the humid air alone due to the elevated temperature gradients in the layered ice mixture. The diffusion
 795 velocities are related as

796
 797
$$\hat{v}_v = v_v \phi_{ha} \quad , \quad (50)$$

798
 799 where the “hat” is used to reference the humid air alone.

800
 801 The time required to accumulate the mass of Eq. (49) on the bounding upper ice surface is given
 802 by

803
 804
$$\hat{t} = \frac{d}{\hat{v}_v} = \frac{\left(2 L_{ha} + \left(\frac{\gamma_i}{\gamma_v}\right) L_i\right)}{\hat{v}_v} \quad , \quad (51)$$

805
 806 or noting Eqs. (47 & 50),

807
 808
$$\hat{t} = \frac{\tau}{\phi_{ha}} \quad . \quad (52)$$

809
 810 The above shows that diffusion in the layered microstructure is enhanced at all humid air volume
 811 fractions as it takes a longer time to achieve the same mass transfer in humid air alone.

812
 813 If on the other hand, one fixes the time, τ , according to Eq. (47), the total mass crossing the
 814 boundary in the humid air alone is given by

815
 816
$$\hat{m} = \tau \gamma_v \hat{v}_v = \left(\frac{2L_{ha} + L_i \left(\frac{\gamma_i}{\gamma_v}\right)}{v_v}\right) \gamma_v \hat{v}_v$$

 817
 818
$$= \phi_{ha} m \quad . \quad (53)$$

819
 820 Hence, for a fixed time, τ , the mass transfer moving through the system of humid air alone is reduced
 821 compared to the mass transfer in the layered ice/humid air mixture.

822
 823 Using either approach above, diffusion is enhanced in the layered microstructure and the
 824 diffusion coefficient of the layered microstructure may be expressed precisely as
 825 Eq. (23), i.e.,



826
$$D_{lm} = \left(\frac{D_{v-a}}{\phi_{ha}} \right) . \quad (54)$$

827 The above results show that one should not view the time taken by the material point F of water
828 while locked in the ice phase as slowing diffusion. Rather, the ice layer is an enormous reservoir of water
829 vapor, providing a continual source for diffusing water vapor until such time that the point F reaches the
830 upper surface of the ice layer.

831
832 Finally, all of the results in this section were developed without reference to the hand-to-hand
833 mass transfer analogy. However, the hand-to-hand analogy provides an elegant shortcut to the identical
834 results of Eq. (54). This fact may be attributed to either: i) adopting the view of shortened diffusion paths,
835 or ii) adopting the view of an elevated intrinsic velocity as was done in Hansen (2019).

836
837

838 6. Discussion

839 This comment paper demonstrates that hand-to-hand water vapor transport provides an effective
840 model for correctly predicting enhanced diffusion in a layered ice/humid air microstructure. The model is
841 supported by rigorous control volume analyses using both a moving control volume and a fixed control
842 volume. Although the hand-to-hand concept is incredibly valuable, one can dispense with the hand-to-
843 diffusion mechanism and still achieve the same results of enhanced diffusion due to the “reservoir effect”
844 of the ice phase holding massive amounts of water vapor. In brief, *the existing ice phase within the*
845 *layered microstructure is a major contributing factor to the overall mass transport of water moving*
846 *through the system*. The approach of Fourteau et al. (2021a) ignores the contribution of mass diffusion
847 attributed to the reservoirs of water vapor contained within the ice layers.

848 The displacement time history seen in Figures 11 also demonstrates that there is no counterflux of
849 mass transfer due to a downward motion of the ice phase. Indeed, there is no negative motion of a
850 material point of water at any time, either in the ice phase or the humid air phase. While point F is locked
851 in the ice phase with no motion, the ice phase steadily moves lower through deposition from water vapor
852 rising from below, producing the *appearance* of downward motion.

853

854 Let us now return to the known energy flux of the layered microstructure given by Eq. (9) and
855 repeated below as

856

857
$$q_{lm} = - \left(\left(\frac{k_{ha}}{\phi_{ha}} \right) + \left(\frac{D_{v-a}}{\phi_{ha}} \right) u_{sg} \frac{d \gamma_v}{d \theta} \right) \frac{\partial \theta}{\partial x} . \quad (55)$$

858

859 The following observations can be made:

860

- 861 • The thermal conductivity is given by

862

863
$$k_{lm} = \left(\frac{k_{ha}}{\phi_{ha}} \right) \quad (56)$$

864

865 This expression is also precisely the thermal conductivity of humid air within the layered
866 microstructure as the energy flux of the layered microstructure is identical to the energy
867 flux of the humid air constituent.

868



- 869
- Consistent with a rigorous control volume analysis as well as the material point tracking
- 870
- analysis of Section 5.1, the diffusion coefficient is given by
- 871

872

$$D_{lm} = \left(\frac{D_{v-a}}{\phi_{ha}} \right) . \quad (57)$$

873

874 The above also represents the diffusion through the humid air constituent of the layered
875 microstructure. In this sense, the decomposition of Eqs. (56) and (57) are identical to the
876 results for humid air as a pure substance put forth by Bird et al. (1960) and outlined in
877 Section 2.2.

878

879 A hand-to-hand model of water vapor transport produces the correct diffusion coefficient.
880 Although the hand-to-hand description of Yosida (1955) is visually superb (outstanding in this writer's
881 view), one could dispense with this concept in favor of the "reservoir effect" of water vapor transport.
882 The reservoir effect has the desirable trait that the "nonphysical" nature of hand-to-hand water vapor
883 diffusion is eliminated.

884

885 Equation (57) shows that diffusion in the layered microstructure is enhanced at all volume
886 fractions compared to diffusion in humid air as a pure substance. The sublimation and deposition of water
887 vapor across ice grains in snow is also clearly present during temperature gradient metamorphism of snow
888 as it leads to microstructural evolution. **Hence, it is entirely possible, indeed probable, for macroscopic
889 water vapor diffusion to be enhanced in snow compared to diffusion in humid air as a pure substance.**
890 An analysis suggesting this diffusion enhancement was provided in Hansen (2019). Present work by the
891 author suggests that for an ice volume fraction of 0.3, the normalized diffusion coefficient for snow
892 ranges from approximately 0.9-1.3, depending on the degree to which hand-to-hand mass transport is
893 present.

894

895 Efforts to quantify precise values of the diffusion coefficient have been limited by confusion over
896 the definition of this important parameter. The present paper provides the clarity to move forward in a
897 consistent manner.

898

900 References

- 901
- 902 Bird, R. B., Stewart, W. E., and Lightfoot, E.: Transport Phenomena, John Wiley and Sons, New York,
903 1960.
- 904
- 905 Calonne, N., Geindreau, C., and Flin, F.: Macroscopic modeling for heat and water vapor transport in dry
906 snow by homogenization, J. Phys. Chem. B, 118, 13393-13403, <https://doi.org/10.10221/jp5052535>,
907 2014.
- 908
- 909 Colbeck, S.: The vapor diffusion coefficient for snow, Water Resour. Res., 29, 109–115,
910 <https://doi.org/10.1029/92WR02301>, 1993.
- 911
- 912 Foslien, W.E.: A Modern Mixture Theory Applied to Heat and Mass Transfer in Snow. M.S. thesis,
913 University of Wyoming, 1994.
- 914
- 915 Fourteau, K., Domine F., and P. Hagenmuller.: Macroscopic water vapor diffusion is not enhanced in
916 snow, Preprint. Discussion, The Cryosphere, <https://doi.org/10.5194/tc-2020-183>, 2021a.
- 917



918 Fourteau, K., Domine F., and P. Hagenmuller.: Impact of water vapor diffusion and latent heat on the
919 effective thermal conductivity of snow, Preprint. Discussion, The Cryosphere, [https://doi.org/10.5194/tc-](https://doi.org/10.5194/tc-2020-317)
920 [2020-317](https://doi.org/10.5194/tc-2020-317), 2021b.
921
922 Giddings, J.C. & E. LaChapelle.: The formation rate of depth hoar. J. Geophys. Res., 67 (6), 2377-2383,
923 1962.
924
925 Hansen, A. C. and Foslien, W.: A macroscale mixture theory analysis of deposition and sublimation rates
926 during heat and mass transfer in dry snow, The Cryosphere, 9, 1857–1878, [https://doi.org/10.5194/tc-9-](https://doi.org/10.5194/tc-9-1857-2015)
927 [1857-2015](https://doi.org/10.5194/tc-9-1857-2015), 2015.
928
929 Hansen, A. C.: Revisiting the vapor diffusion coefficient in dry snow, Preprint. Discussion, The
930 Cryosphere, <https://doi.org/10.5194/tc-2019-143>, 2019.
931
932 Shertzer, R.H. and E.E. Adams.: A Mass Diffusion Model for Dry Snow Utilizing a Fabric Tensor to
933 Characterize Anisotropy, J. Advances in Modeling Earth Systems, 2018.
934
935 Sommerfeld, R., Friedman, I., and Nilles, M.: The fractionation of natural isotopes during temperature
936 gradient metamorphism of snow, in: The Fractionation of Natural Isotopes During Temperature Gradient
937 Metamorphism of Snow, 95–105, D. Reidel Publishing, Boston, 1987.
938
939 Sonin, A.A.: Fundamental laws of motion for particles, material volumes, and control volumes, MIT,
940 https://web.mit.edu/2.25/www/pdf/fundamental_laws.pdf, 2003.
941
942 Yosida, Z.: Physical studies of deposited snow: thermal properties I, Tech. rep., Institute of low
943 temperature science, Hokkaido University, Japan, 1955.
944
945

946 Nomenclature

948 Latin Letters

949	D	diffusion coefficient
950	k	thermal conductivity
951	n	unit normal
952	q	energy flux
953	t	time
954	u_{sg}	latent heat of sublimation of ice
955	v	velocity
956	x	macroscale coordinate

959 Greek Symbols

960	ξ	microscale coordinate
961	γ_v	density of vapor component
962	ρ	density
963	θ	absolute temperature
964	ϕ_α	volume fraction of constituent α

966 Superscripts

967	(c)	conduction
-----	-----	------------



- 968 (d) diffusion
- 969
- 970 **Subscripts**
- 971 C reference frame moving with ice front
- 972 f advancing ice front due to ice accretion
- 973 i ice constituent
- 974 ha humid air constituent
- 975 lm layered microstructure
- 976 v vapor component within humid air
- 977 v-a water vapor in air
- 978 s snow
- 979
- 980



981 **List of Figures**

982

983 **Figure 1.** Water vapor transport mechanisms in snow exhibiting: a) hand-to-hand water vapor transport
984 (red arrows) involving continuous sublimation and condensation of water vapor and, b) water
985 vapor passing around ice grains (green arrows).
986

987 **Figure 2.** (a) Layered ice/humid air microstructure shown in green bounded by solid ice blocks. (b) A
988 macroscale continuum point of the layered microstructure showing the presence of both ice and
989 humid layers.
990

991 **Figure 3.** Arbitrary fixed region \mathcal{R} showing a surface flux of the vector field, F , leaving the boundary
992 defined by the surface, $\partial\mathcal{R}$.
993

994 **Figure 4.** A comparison of the exact and approximate forms of the normalized energy flux of the layered
995 microstructure. Note that the exact energy flux converges to the known energy flux for the case
996 of solid ice.
997

998 **Figure 5.** (a) Layered microstructure shown in green bounded by solid ice *blocks*. (a) Coincident fixed
999 and moving control volumes at time $t = 0$, shown by the dashed line. (b) Fixed control volume
1000 (red) and moving control volume (green) advancing with the ice front at time t .
1001

1002 **Figure 6.** (a) Humid air as a pure substance under a temperature gradient showing an advancing ice front
1003 of length ℓ occurring in a characteristic time τ . (b) A layered microstructure with ice volume
1004 fraction $\phi_i = 1/3$ showing an advancing ice front of length 1.5ℓ occurring in the same
1005 characteristic time τ as for humid air alone shown in (a)—see the discussion in Section 4.2.
1006

1007 **Figure 7.** (a) Unit cell with a moving control volume that advances downward with the moving ice front
1008 cause by ice accumulation on the lower surface of the ice constituent. (b) Alternate
1009 configuration of the unit cell where the moving control volume extends through the middle of
1010 the ice phase.
1011

1012 **Figure 8.** Fixed control volume showing a unit cell with: (a) the ice phase at time $t = 0$, and (b) the ice
1013 phase at a later time, t .
1014

1015 **Figure 9.** (a) Fixed control volume of characteristic length 1.5ℓ , filling with the advancing ice front in
1016 time τ , (b) Fixed control volume enclosing the lower solid ice/ice mixture boundary where
1017 sublimation is occurring.
1018

1019 **Figure 10.** Vertical displacement versus time for two material points of water. At time t' , the ice phase
1020 has turned over entirely showing the apparent downward motion of ice while the mass flux is
1021 monotonically increasing (nonnegative) for all time.
1022

1023 **Figure 11.** Motion of a continuum material point, F , of water as it traverses through humid air, is locked
1024 within an ice layer, and then is released via sublimation to again traverse through humid air to
1025 reach the upper boundary of solid ice.
1026



fig01

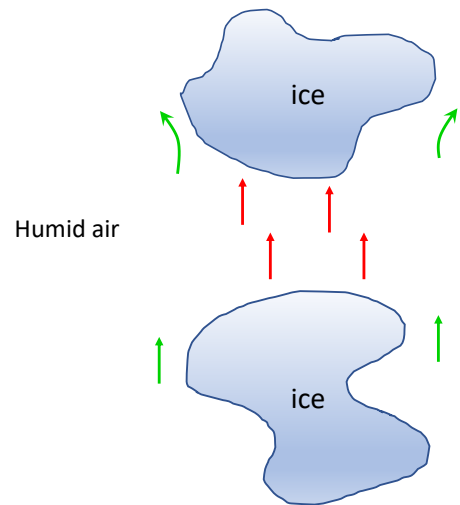




fig02

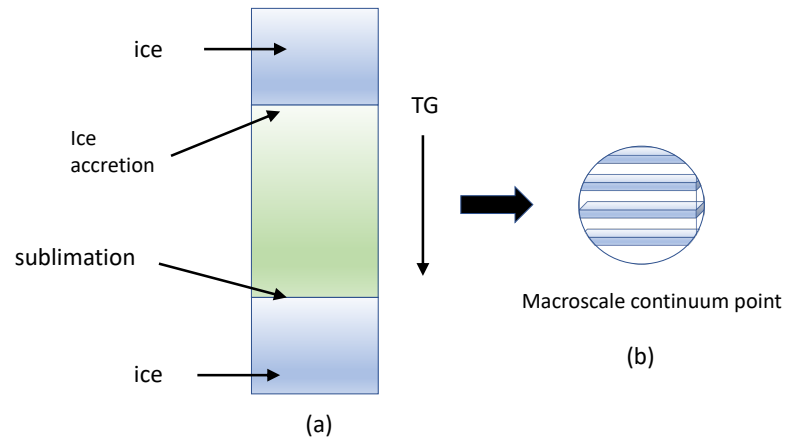




fig03

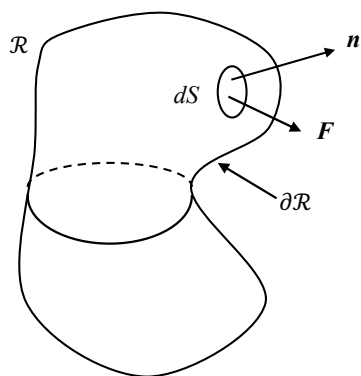




fig04

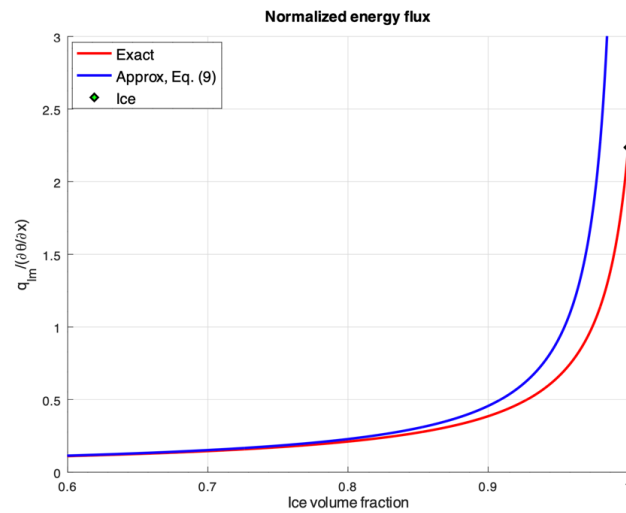




fig05

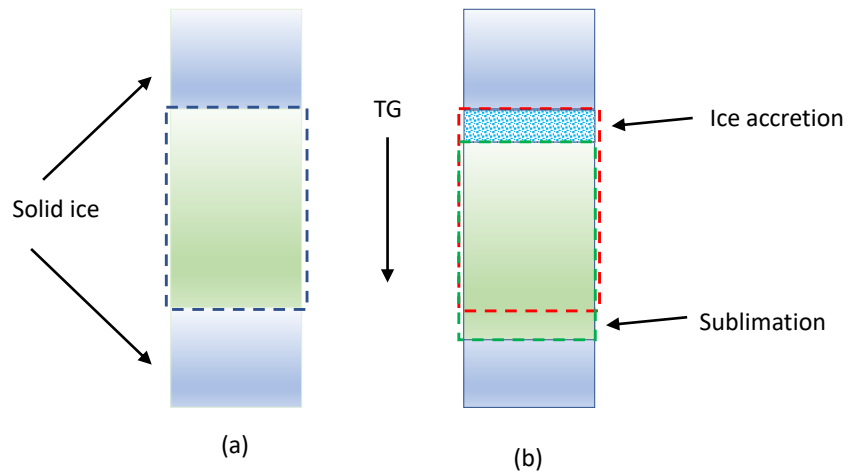




fig06

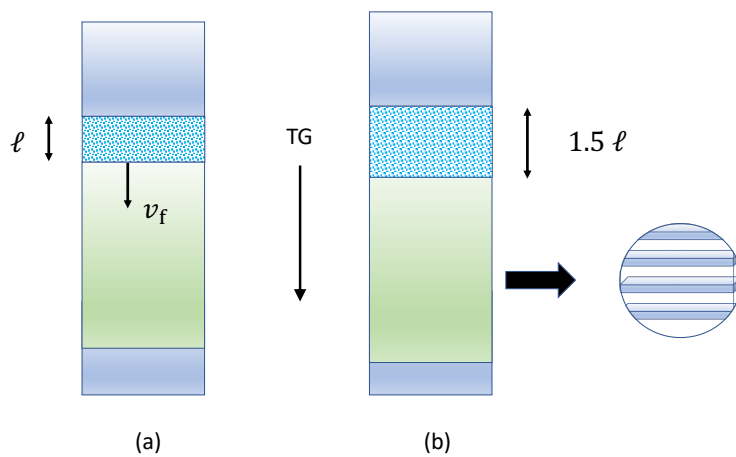




fig07

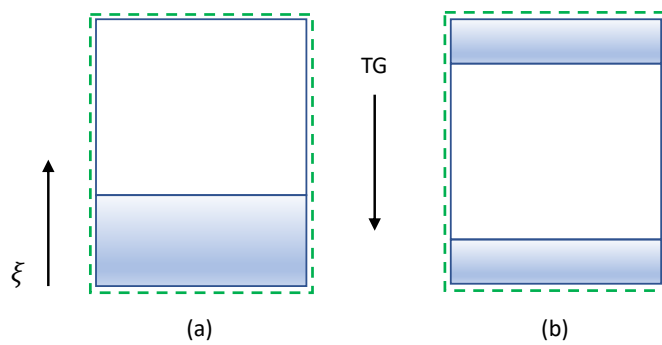




fig08

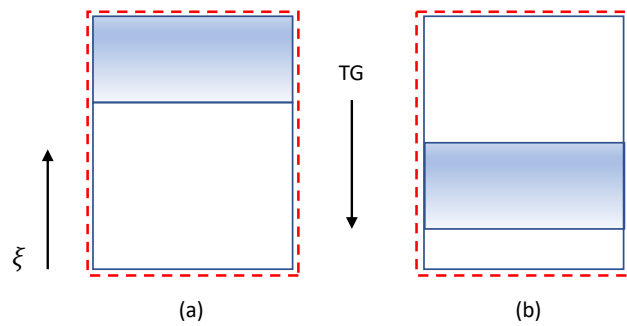




fig09

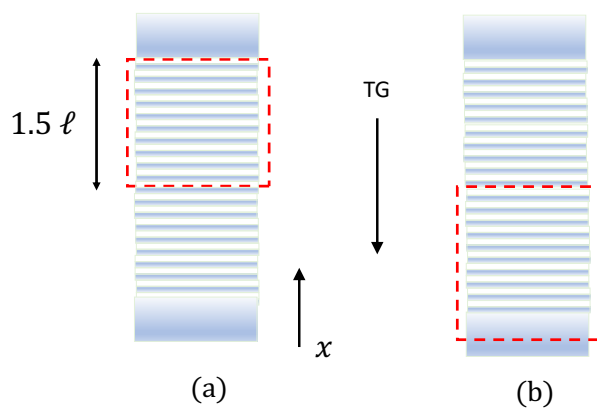




fig10

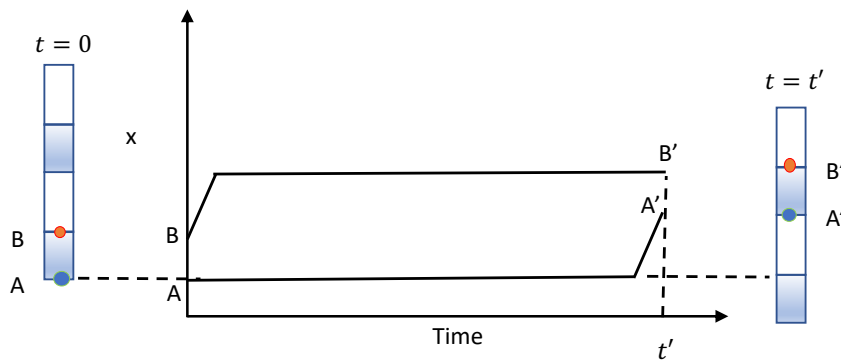




fig11

